Journal of Nuclear Medicine, published on March 13, 2020 as doi:10.2967/jnumed.119.241109

^{68}Ga-PSMA guided bone biopsies for molecular diagnostics in metastatic prostate cancer patients

Anouk C. de Jong, MD[1,2*], Minke Smits, MD[3*], Job van Riet, BSc[1,4], prof. Jurgen J. Fütterer, MD, PhD[5], Tessa Brabander, MD, PhD[2], Paul Hamberg, MD, PhD[6], Inge M. van Oort, MD PhD[7], prof. Ronald de Wit, MD, PhD[1], Martijn P. Lolkema, MD, PhD[1], Niven Mehra, MD, PhD[3], Marcel Segbers, MSc[2#], Astrid A.M. van der Veldt, MD, PhD[1,2#]

*Shared first author, #Shared last author

[1] Department of Medical Oncology, Erasmus MC Cancer Institute, Rotterdam, The Netherlands; [2] Department of Radiology & Nuclear Medicine, Erasmus MC, Rotterdam, The Netherlands; [3] Department of Medical Oncology, Radboud UMC, Nijmegen, The Netherlands; [4] Cancer Computational Biology Center, Erasmus MC Cancer Institute, Rotterdam, The Netherlands; [5] Department of Radiology and Nuclear Medicine, Radboud UMC, Nijmegen, The Netherlands; [6] Department of Internal Medicine, Franciscus Gasthuis & Vlietland, Rotterdam, The Netherlands; [7] Department of Urology, Radboud UMC, Nijmegen, The Netherlands.

Corresponding author: A.A.M. van der Veldt, Department of Medical Oncology, Erasmus MC Cancer Institute, Dr. Molewaterplein 40, 3015 GD Rotterdam, The Netherlands. Tel: +31 (0)10 704 17 54. Fax: +31 (0)10 704 10 03. E-mail address: a.vanderveldt@erasmusmc.nl

First authors:

1. A.C. de Jong, MD, PhD candidate, Department of Medical Oncology, Erasmus MC Cancer Institute, Dr. Molewaterplein 40, 3015 GD Rotterdam, The Netherlands. Tel: +31 (0)10 704 4375. Fax: +31 (0)10 704 10 03. E-mail address: a.c.dejong@erasmusmc.nl

2. M. Smits, MD, PhD candidate, Department of Medical Oncology, Radboud UMC, Geert Grooteplein Zuid 10, 6525 GA Nijmegen, The Netherlands. Tel: +31 (0)24 361 03 53. E-mail address: m.smits@radboudumc.nl

This work was presented at the European Society for Medical Oncology 2019 in Barcelona and selected as winner of Best Poster Award at ESMO 2019.

Word count abstract: 297

Word count total manuscript: 5583

Financial support is not applicable. For brevity, the disclaimer is listed once at the end of the manuscript.

Short running title: ^{68}Ga-PSMA guided bone biopsies

ABSTRACT

For individual treatment decisions in patients with metastatic prostate cancer (mPC), molecular diagnostics are increasingly used. Bone metastases are frequently the only source for obtaining metastatic tumor tissue. However, the success rate of computed tomography (CT)-guided bone biopsies for molecular analyses in mPC patients is only ~40%. Positron emission tomography (PET) using Gallium-68 prostate specific membrane antigen (^{68}Ga-PSMA) is a promising tool to improve the harvest rate of bone biopsies for molecular analyses. Aim of this study was to determine the success rate of ^{68}Ga-PSMA guided bone biopsies for molecular diagnostics in mPC patients. **Methods**: Within a prospective multicenter whole-genome sequencing trial (NCT01855477), 69 mPC patients underwent ^{68}Ga-PSMA PET/CT prior to bone biopsy. Primary endpoint was success rate (tumor percentage ≥30%) of ^{68}Ga-PSMA guided bone biopsies. At biopsy sites, ^{68}Ga-PSMA uptake was quantified using rigid body image registration of ^{68}Ga-PSMA PET/CT and interventional CT. Actionable somatic alterations were identified. **Results**: Success rate of ^{68}Ga-PSMA guided biopsies for molecular analyses was 70%. At biopsy sites categorized as positive, inconclusive, or negative for ^{68}Ga-PSMA uptake, 70%, 64%, and 36% of biopsies were tumor positive (≥30%), respectively (p=0.0610). In tumor positive biopsies, ^{68}Ga-PSMA uptake was significantly higher (p=0.008), whereas radiodensity was significantly lower (p=0.006). With an area under the curve of 0.84 and 0.70, both ^{68}Ga-PSMA uptake (maximum standardized uptake value) and radiodensity (mean Hounsfield Units) were strong predictors for a positive biopsy. Actionable somatic alterations were detected in 73% of the sequenced biopsies. **Conclusion:** In patients with mPC, ^{68}Ga-PSMA PET/CT improves the success rate of CT-guided bone biopsies for

molecular analyses, thereby identifying actionable somatic alterations in more patients. Therefore, ^{68}Ga-PSMA PET/CT may be considered for guidance of bone biopsies in both clinical practice and clinical trials.

Keywords: bone biopsy, ^{68}Ga-PSMA-PET, molecular diagnostics, whole genome sequencing, prostate cancer.

INTRODUCTION

With more than 350,000 men dying of prostate cancer in 2018, prostate cancer is not only one of the most common malignancies in men, but also the fifth leading cause of cancer-related death worldwide*(1)*. To improve treatment planning for individual patients with metastatic prostate cancer (mPC), molecular analyses are increasingly used to predict treatment response, guide clinical decision making and identify additional targets for targeted therapy*(2-4)*. Due to tumor evolution and genetic adaption following castration resistance and subsequent treatment resistance, tumor DNA for molecular analyses is preferably obtained from a biopsy of a metastatic lesion. As bone-only and bone predominant disease are most frequently reported in patients with mPC, bone metastases are usually the only source for molecular analyses*(5-6)*.

In men with mPC, 67-77% of bone biopsies have sufficient quality for diagnostic histopathological examination*(7-9)*. However, molecular analyses on CT-guided bone biopsies from prostate cancer are less feasible, as the success rate is only 39-44% and 36.5% for RNA analysis and whole exome sequencing, respectively*(7, 8, 10)*. This poor success rate of bone biopsies might be due to the predominantly osteoblastic character of these metastases. As bone metastases of prostate cancer have a dense sclerotic matrix and decreased tumor cellularity, these lesions are difficult to distinguish from non-malignant osteosclerosis on CT*(11)*.

In clinical practice, most bone biopsies are guided by computed tomography (CT). Since the yield of CT-guided bone biopsies for molecular analyses is rather low, the use of molecular diagnostics for personalized treatment in prostate cancer patients is limited. To improve the yield of bone biopsies in mPC patients, biopsies could be obtained from

bone metastases, which express prostate specific membrane antigen (PSMA). In the apical region of normal prostate cells, PSMA shows physiological expression, whereas it is usually 100-1000x overexpressed in prostate cancer cells*(12)*. To visualize and quantify PSMA expression *in vivo*, positron emission tomography (PET) using Gallium-68 PSMA (^{68}Ga-PSMA) can be performed. Nowadays, ^{68}Ga-PSMA PET/computed tomography (CT) is increasingly used in the setting of biochemical recurrence, as it has a high sensitivity and specificity for early detection of prostate cancer*(13)*. Recently, fused images of ^{68}Ga-PSMA PET/CT and diffusion weighted MRI, in combination with cone-beam CT guidance, have been applied to guide bone biopsies in patients with prostate cancer. Though in a small number of patients (N=10), this pilot study showed a success rate of 80%*(14)*. Therefore, ^{68}Ga-PSMA PET/CT is a promising technique to increase the success rate of bone biopsies for molecular analyses in prostate cancer patients.

Within a prospective multicenter whole-genome sequencing (WGS) trial, we determined the success rate of ^{68}Ga-PSMA guided bone biopsies for molecular diagnostics in metastatic prostate cancer patients. In addition, we evaluated the potential impact of these molecular analyses on clinical decision making in mPC patients.

MATERIALS AND METHODS

Design

In this comprehensive PET study, mPC patients, who had a ^{68}Ga-PSMA guided bone biopsy within the prospective multicenter nationwide CPCT-02 study (NCT01855477), were included*(15)*. CPCT-02 aims to improve selection of patients for experimental therapy by WGS of tumor DNA, which is obtained by image-guided biopsies. For the

current study, informed consent was obtained within CPCT-02, and additional approval was provided by the institutional review boards of two academic institutes in the Netherlands: Erasmus Medical Center in Rotterdam (EMC) and Radboud University Medical Center in Nijmegen (RUMC).

Patients

Between December 2014 and July 2018, all mPC patients, who underwent ^{68}Ga-PSMA PET/CT within 12 weeks prior to a completed bone biopsy procedure within CPCT-02, were included. Full in- and exclusion criteria of CPCT-02 were described previously*(15)*. Tumor tissue was obtained from a metastatic lesion to fully capture the genomic tumor evolution. Patients could be included at multiple time points in their treatment course, resulting in repeated biopsies for some patients. Biopsies were always obtained prior to the start of a new systemic treatment. Clinical data were collected in an electronic case report form (ALEA Clinical).

Primary and Secondary Endpoints

Primary endpoint was the success rate of ^{68}Ga-PSMA guided bone biopsies in patients with mPC, with success defined as ≥30% tumor cells in at least one biopsy core (i.e. the minimal amount of tissue required for DNA isolation for WGS), as assessed by a dedicated pathologist. Exploratory endpoints included the correlation between biopsy success and imaging (standardized uptake value [SUV] and Hounsfield Units [HU]) and laboratory variables (haemoglobin [Hb], alkaline phosphatase [ALP], prostate specific antigen [PSA],

and lactate dehydrogenase [LDH]). In addition, the potential impact of molecular analyses on clinical decision making was evaluated.

Image Acquisition

Prior to the biopsy procedure, ^{68}Ga-PSMA PET/CT was performed to identify a biopsy site with high ^{68}Ga-PSMA uptake. During the procedure, biopsies were performed with or without CT, or ultrasound guidance, based on the interventional radiologist's decision.

^{68}Ga-PSMA PET and Low Dose CT. On-site, PSMA-HBED-CC was labelled with ^{68}Ga and administered intravenously with a mean (± SD) single bolus of 133 ± 35 MBq 68Ga-PSMA-HBED-CC. At 60 minutes post injection, images were acquired from head to mid-thigh on a Biograph mCT PET/CT scanner (Siemens Healthineers, Erlangen, Germany). A low-dose CT was acquired with 120kV and 40 reference mAs (EMC) or 50 reference mAs (RUMC). All PET data were obtained during 3 minutes per bed position, except for images with 4 minutes per bed position for patients with weight >70 kg in EMC. For quantitative analyses of ^{68}Ga-PSMA uptake, data were reconstructed according to Evaluation and Report Language*(16).*

Interventional CT. Prior to CT acquisition for CT-guided biopsy, the field of view was determined by acquiring an overview image. Next, subsequent CT scans with a smaller field of view were acquired to visualize the biopsy needle until the biopsy site was reached.

Biopsy Procedure

Bone biopsies were performed according to local institutional guidelines. The biopsy site was selected by the interventional radiologist based on clinical judgement, safety, and prior imaging including ^{68}Ga-PSMA PET/CT.

Image Analyses

Rigid Body Image Registration. In order to evaluate whether biopsies were accurately obtained from a ^{68}Ga-PSMA positive lesion, co-registration of ^{68}Ga-PSMA PET/CT and the interventional CT was retrospectively performed using rigid body image registration. This analysis, which was performed with the Elastix Toolbox*(17, 18)*, enables measurement of ^{68}Ga-PSMA uptake at the exact position of the biopsy site. When the image quality of ^{68}Ga-PSMA PET, low-dose CT and interventional CT was sufficient for rigid body image registration, patients were included for this exploratory analysis. Rigid body image registration merges ^{68}Ga-PSMA PET/CT and the interventional CT within two steps. To exclude soft tissues in both image registration steps, bone masks were obtained by applying a region growing algorithm that included CT voxels >150 HU. In the first co-registration step, patient motion on interventional CT is corrected by co-registration of the overview image and the image acquired during biopsy. Next, the overview image of the interventional CT was co-registered with the low-dose CT of the ^{68}Ga-PSMA PET/CT image. Combining rotation calculations from both image registration steps with interventional CT enabled fusion of ^{68}Ga-PSMA PET with the interventional CT, thereby visualizing the biopsy needle.

^{68}Ga-PSMA Uptake and Radiodensity at Biopsy Site. An experienced nuclear medicine physician (T.B.), who was blinded for the biopsy results, determined visually whether the biopsy was accurately taken from a ^{68}Ga-PSMA positive lesion, using a three-point scale categorized as hit, borderline or miss. Besides these qualitative analyses, quantitative analyses consisted of SUV and HU measurements. To measure ^{68}Ga-PSMA uptake (SUV) and radiodensity (HU) at the exact biopsy location, a cylindrical volume of interest

(VOI) with a length of 2 cm and a diameter of 1 cm was drawn at the site of the biopsy as visualized on rigid body co-registration images of ^{68}Ga-PSMA PET and interventional CT. VOIs were defined in Python using in-house developed scripts, based on SimpleITK framework for medical imaging (19). The maximum and mean SUV of ^{68}Ga-PSMA uptake were calculated using the injected radioactivity, body weight and the amount of radioactivity within a VOI. To assess radiodensity in bone metastases, HUs were determined on CT images. For CT measurements, if necessary, VOIs were minimally moved or reduced in size to avoid overlap with cortical bone.

Molecular Analyses

Alterations in genes described in OncoKB, a precision oncology knowledge base, were extracted from the genomic data of all successfully sequenced biopsies and categorized as level 1, 2, 3, or 4 alterations, based on available (clinical) evidence*(20)*. In addition, PTEN deletions were extracted as these might also be actionable with AKT-inhibitors*(2)*. Genomic analyses are described in detail in the Supplementary*(20-27)*.

Statistical Analyses

Depending on normality distribution, the unpaired t-test or Mann-Whitney U test was used to test for differences between clinical variables (age, Gleason score, haemoglobin, ALP, LDH, and PSA), imaging variables (HU_{mean}, HU_{max}, SUV_{mean}, and SUV_{max}), and primary outcome of biopsy (≥30% tumor). To test for differences between the summed Gleason score (<8 and ≥8) and primary outcome, a Chi-square test was used. The three ^{68}Ga-PSMA uptake categories (hit, borderline, miss) were compared for tumor positivity (≥30% tumor) using the Chi-square for trend test. For SUV at the biopsy location, the three

biopsy outcome groups were compared using the Kruskal-Wallis test in combination with Dunn's multiple comparisons test. Univariate and multivariate regression analyses were performed to evaluate relations between variables and primary outcome. For these analyses all non-normal distributed variables were log-transformed prior to testing. Since normal distribution was not reached for LDH by log-transformation, LDH was categorized in normal LDH (<250) and elevated (≥250) and a Chi-square test was used to test for an association with biopsy outcome. Univariate logistic regression analysis tested for any association between continuous variables and primary outcome. Subsequently, significantly associated variables were selected for multivariate logistic regression analysis. Due to the relatively small sample size, the most significant variables of HU (mean or max) and SUV (mean or max) were selected for multivariate testing. No correction was set for multiplicity of secondary endpoints. Odds for a positive biopsy were calculated by logistic regression for SUV and HU. For the area under the curve and receiver operating characteristic curve, the logarithm of odds was calculated. Receiver operating characteristic curves were calculated for HU_{mean} and SUV_{max}. All statistical tests were performed two-sided. A p-value of ≤0.05 was considered statistically significant.

RESULTS

Biopsy Selection

Between December 2014 and June 2018, 115 bone biopsies from 103 patients with mPC were obtained within CPCT-02 in EMC and RUMC. Prior to 71 biopsies (62%), ^{68}Ga-PSMA PET/CT was performed to identify bone metastases, while 44 biopsies (38%) within CPCT-02 were preceded by other imaging modalities. Two out of 71 ^{68}Ga-PSMA guided

biopsies (3%) were not eligible because of a failed biopsy procedure and >12 weeks between imaging and biopsy. In total, 69 ^{68}Ga-PSMA guided biopsies, from 60 individual patients, were eligible for primary analysis to determine the success rate of ^{68}Ga-PSMA guided bone biopsies (Fig. 1). Seven patients underwent two ^{68}Ga-PSMA guided bone biopsies. One patient underwent three ^{68}Ga-PSMA guided bone biopsies. Median time between ^{68}Ga-PSMA PET/CT and the biopsy procedure was nine days (interquartile range 3-22).

Clinical Characteristics and Success Rate of ^{68}Ga-PSMA Guided Biopsies

The clinical characteristics of patients and biopsies are described in Table 1. Biopsies were primarily performed in the castration resistant setting (97%, N=67) and most commonly obtained from the pelvis (N=57, 83%). During the procedure, biopsies were performed unguided (N=5, 7%), or guided by ultrasound (N=1, 1%), or CT (N=63, 91%), based on the interventional radiologist's decision. During one biopsy procedure (1%), excessive bleeding, which was directly controlled by manual pressure, occurred.

Based on tumor percentage (≥30%) in at least one core, 48 out of 69 (70%) ^{68}Ga-PSMA guided biopsies (44 out of 60 individual patients (73%)) were eligible for molecular analyses. No significant differences were found in age (p=0.42), Gleason score (p=0.46) and baseline laboratory findings (Hb p=0.54, PSA p=0.36, ALP p=0.56) between biopsies with tumor percentage <30% and ≥30%, although elevated LDH levels were seen with borderline significance in the group with a successful biopsy (p=0.05). In the univariate logistic regression analysis, none of these variables were associated with biopsy outcome (data not shown). The success rate of biopsies obtained from pelvis (N=57, 83%), spine (N=6, 9%), and other locations (N=6, 9%) was 65%, 100% and 83%, respectively.

^{68}Ga-PSMA Uptake and Radiodensity at Biopsy Site

To evaluate whether biopsies were accurately obtained from lesions with high ^{68}Ga-PSMA uptake, ^{68}Ga-PSMA PET/CT was co-registered with interventional CT (Figs. 2a-d) for qualitative and quantitative analyses (Fig.1). For 55 biopsies, rigid body image registration could be performed adequately (Fig. 1). Based on the rigid body image registrations, 33 biopsies were categorized as hit, 11 biopsies as borderline, and 11 biopsies as miss (Fig. 3a). As expected, biopsy sites categorized as hit had higher SUV_{max} and SUV_{mean} compared with biopsy sites categorized as miss ($p<0.001$ for both) (Figs. 3b-c). Subsequently, the correlation between ^{68}Ga-PSMA uptake and biopsy outcome was evaluated. At biopsy sites categorized as hit, borderline or miss for ^{68}Ga-PSMA uptake, 70%, 64%, and 36% of biopsies were tumor positive (≥30%), respectively ($p=0.0610$, Fig. 3a).

At biopsy sites with tumor percentage ≥30%, median ^{68}Ga-PSMA uptake was significantly higher (SUV_{max} 20.9, inter quartile range [IQR] 10.0-32.1; SUV_{mean} 10.3, IQR 3.4-18.7), whereas median ^{68}Ga-PSMA uptake was lower at biopsy sites with tumor percentage <30% (SUV_{max} 6.7, IQR 3.7-14.2; SUV_{mean} 3.4, IQR, 1.8-9.1; $p=0.0021$ and $p=0.0123$, respectively) (Figs. 4a-b). In contrast, median radiodensity on CT was significantly lower at biopsy sites with tumor percentage ≥30% (HU_{max} 786, IQR 600-977; HU_{mean} 294, IQR 184-473) as compared to biopsy sites with tumor percentage <30% (HU_{max} 1019, IQR 780-1132; HU_{mean} 524, IQR 296-738; $p=0.0266$ and $p=0.0064$, respectively) (Figs. 4c-d). In univariate logistic regression analysis, SUV and HU values were also significantly associated with biopsy outcome (SUV_{max} $p= 0.008$, SUV_{mean} $p=0.016$, HU_{mean} $p= 0.006$, and HU_{max} $p=0.037$) (Supplemental Table 1a). After stepwise

multivariate analysis, HU_{mean} and SUV_{max} resulted in an odds ratio of 0.995 (95%CI 0.992-0.998, p=0.003) and 11.737 (95%CI 2.258-60.996, p=0.003), respectively (Supplemental Table 1b). Receiver operating characteristic curves of HU_{mean} and SUV_{max} for successful biopsies had an area under the curve of 0.70 and 0.84, respectively (Supplemental Fig. 1).

Clinical Impact of ^{68}Ga-PSMA Guided Bone Biopsies for Molecular Analyses

Forty out of 48 positive biopsies (83%) were successfully used for WGS (Fig. 1). Median *in silico* tumor purity of the successfully sequenced samples was 55% (range 17-94%) (Supplemental Fig. 2)*(20-27).* In total, 53 actionable somatic alterations were detected in 73% (N=29) of the successfully sequenced biopsies (Fig. 5). Forty-one actionable somatic alterations, detected in 21 biopsies, were described in the OncoKB database as level 1 (n=9, 22%), level 2 (n=4, 10%), level 3 (n=13, 32%), and level 4 (n=15, 37%)*(20)*. Twelve biopsies (30%) contained a deep *PTEN* deletion, which is not (yet) included in the OncoKB database, but might be actionable with AKT-inhibitors*(2)*. The genomic landscape of metastatic castration resistant prostate cancer, including this subset of biopsies, has been described in detail by Van Dessel et al.*(22)*.

DISCUSSION

In this comprehensive PET study, we show that ^{68}Ga-PSMA guided bone biopsies provide sufficient quality for molecular analyses in 70% of the biopsies. Our findings indicate that ^{68}Ga-PSMA guided bone biopsies are more successful than bone biopsies with CT-guidance only, that have a reported success rate for molecular analysis of only

36.5-44% in patients with mPC *(7, 8, 10)*. With 70% of the biopsies being successful for molecular analyses, the success rate approximates the overall success rate of 76.5% for 3655 biopsies within the CPCT-02 study, which mainly included non-skeletal biopsies*(21)*.

For objective analyses of the success rate of ^{68}Ga-PSMA guided bone biopsies, we applied rigid body image registration, which confirmed that the majority of biopsies was accurately obtained from a lesion with high ^{68}Ga-PSMA uptake. In addition, there was a trend towards a higher percentage of tumor positive biopsies in the hit group. For biopsies with a tumor percentage of ≥30%, ^{68}Ga-PSMA uptake was significantly higher than for biopsies with a tumor percentage of <30%. In contrast, HU values on CT were lower for biopsies with a tumor percentage of ≥30% than for biopsies with a tumor percentage of <30%. The higher success rate of biopsies from bone lesions with lower HU values has also been reported by two other studies*(7,8)*, indicating that osteosclerotic lesions with high HU values contain less viable tumor cells. With an area under the curve of 0.84 and 0.70, both SUV_{max} and HU_{mean} were strong predictors for a positive biopsy. In the absence of ^{68}Ga-PSMA PET/CT, it might therefore be advisable to obtain biopsies from less sclerotic lesions with lower HU values.

The high frequency of actionable alterations, found in this study, emphasizes the medical need for a high success rate of bone biopsies. Within the CPCT-02 trial, potentially actionable alterations, identified by WGS of the tumor biopsy, were shared with the patient to enable targeted treatment in, for example, the Drug Rediscovery Protocol (NCT02925234). According to this protocol, patients are treated with approved, off-label targeted agents based on the molecular characteristics of the tumor. First results are promising with clinical benefit for multiple treatment cohorts*(28)*.

As ^{68}Ga-PSMA PET is increasingly and widely available in current clinical practice, it can be easily implemented to improve the success rate of bone biopsies. By optimizing the first step of the pipeline for molecular diagnostics, ^{68}Ga-PSMA PET significantly contributes to improved genomic characterization of mPC.

Although the current study shows a high success rate, there are a few limitations of ^{68}Ga-PSMA guided bone biopsies for molecular diagnostics. First, tumor heterogeneity might be better reflected by molecular analyses of liquid biopsies than by WGS of tumor tissue from a single lesion. However, techniques for detailed molecular analyses of liquid biopsies are still under development, while WGS of tissue biopsies is currently more feasible. Second, PSMA expression has high inter- and intra-patient heterogeneity*(29)*. High PSMA expression is associated with defective DNA damage repair and PTEN loss, whereas patients with low ^{68}Ga-PSMA expression have poor survival*(29-31)*. Since bone biopsies in this study were not obtained from metastases with low ^{68}Ga-PSMA uptake, these sites are underrepresented in the current study.

In addition, there were some notable results. First, four biopsies that were scored as miss (^{68}Ga-PSMA negative) did contain ≥30% tumor cells (false negative). As these biopsies were all close to a ^{68}Ga-PSMA positive lesion, these false negative results may be due to patients' movements and/or different spatial resolution between scans. Although the majority of biopsies was accurately obtained from lesions with high ^{68}Ga-PSMA uptake, guidance might be further optimized by real-time visualization of ^{68}Ga-PSMA uptake, though this is technically and logistically more challenging.

Second, in five biopsies, which were all obtained from spine or ribs, image registration failed. This image registration failure at non-pelvic sites may be explained by the rigid body algorithm, which relies on the assumption that the spine and rib cage are rigid

bodies. As the rigid body algorithm was only applied for image analyses in this study, this limitation will not impact the feasibility of ^{68}Ga-PSMA guided biopsies from non-pelvic sites in clinical practice.

CONCLUSION

In conclusion, ^{68}Ga-PSMA guided bone biopsies have a 70% success rate for molecular analyses in mPC patients, indicating that ^{68}Ga-PSMA PET/CT has added value to increase the success rate of CT-guided bone biopsies. In successful ^{68}Ga-PSMA guided biopsies, whole genome sequencing identified numerous targetable mutations, emphasizing the potential clinical impact of ^{68}Ga-PSMA guided bone biopsies in mPC patients.

DISCLOSURE

Funding was not applicable. A.C. de Jong, M. Smits, J. van Riet, T. Brabander, P. Hamberg and M. Segbers declare that they have no competing interests. J. Fütterer received speaker fees from Astellas and Siemens, and received institutional research support from Siemens. I.M. van Oort received speaker fees from Astellas, Janssen, Bayer, MDxHealth and Sanofi. R. de Wit received advisory fees from Sanofi, Merck, Bayer, Roche, Janssen and Clovis, speaker fees from Sanofi and Merck and institutional research grants from Sanofi and Bayer. M. Lolkema received institutional research funding from Johnson & Johnson and Astellas. N. Mehra played an advisory role (both institutional as personal) for Roche, MSD, Bayer, Astellas and Janssen, received research support (institutional) from Astellas, Janssen, Pfizer, Roche and Sanofi, Genzyme and

travel support from Astellas, MSD. A.A.M. van der Veldt is a member of the advisory board of BMS, MSD, Roche, Novartis, Pierre Fabre, Pfizer, Sanofi and Ipsen. No other potential conflicts of interest relevant to this article exist.

ACKNOWLEDGEMENTS

We thank, S. Klein and A. Moelker for their contribution to the rigid body image registration analysis, M. Simons for help with the molecular analyses, A. Rieborn and W. Onstenk for help with collecting data, and E. Oomen - de Hoop for statistical advice.

KEY POINTS

QUESTION: What is the success rate of ^{68}Ga-PSMA guided bone biopsies for molecular analyses in metastatic prostate cancer patients?

PERTINENT FINDINGS: Within a prospective multicenter whole-genome sequencing trial (NCT01855477), 69 metastatic prostate cancer patients underwent ^{68}Ga-PSMA PET/CT prior to bone biopsy. The success rate of ^{68}Ga-PSMA guided bone biopsies for molecular analyses was 70%.

IMPLICATIONS FOR PATIENT CARE: In patients with metastatic prostate cancer, ^{68}Ga-PSMA PET/CT improves the success rate of CT-guided bone biopsies for molecular analyses, thereby identifying actionable somatic alterations in more patients.

REFERENCES

1. Bray F, Ferlay J, Soerjomataram I, Siegel RL, Torre LA, Jemal A. Global cancer statistics 2018: GLOBOCAN estimates of incidence and mortality worldwide for 36 cancers in 185 countries. *CA Cancer J Clin.* 2018;68:394-424.

2. de Bono JS, De Giorgi U, Rodrigues DN, et al. Randomized phase II study evaluating AKT Blockade with ipatasertib, in combination with abiraterone, in patients with metastatic prostate cancer with and without PTEN Loss. *Clin Cancer Res*. 2019;25:928-936.

3. Mateo J, Carreira S, Sandhu S, et al. DNA-repair defects and olaparib in metastatic prostate cancer. *N Engl J Med*. 2015;373:1697-1708.

4. Abida W, Cheng ML, Armenia J, et al. Analysis of the prevalence of microsatellite instability in prostate cancer and response to immune checkpoint blockade. *JAMA Oncol*. 2019;5:471-478.

5. Halabi S, Kelly WK, Ma H, et al. Meta-analysis evaluating the impact of site of metastasis on overall survival in men with castration-resistant prostate cancer. *J Clin Oncol.* 2016;34:1652-1659.

6. Bubendorf L, Schopfer A, Wagner U, et al. Metastatic patterns of prostate cancer: an autopsy study of 1,589 patients. *Hum Pathol.* 2000;31:578-583.

7. Holmes MG, Foss E, Joseph G, et al. CT-guided bone biopsies in metastatic castration-resistant prostate cancer: factors predictive of maximum tumor yield. *J Vasc Interv Radiol*. 2017;28:1073-1081.

8. Spritzer CE, Afonso PD, Vinson EN, et al. Bone marrow biopsy: RNA isolation with expression profiling in men with metastatic castration-resistant prostate cancer--factors affecting diagnostic success. *Radiology*. 2013;269:816-823.

9. McKay RR, Zukotynski KA, Werner L, et al. Imaging, procedural and clinical variables associated with tumor yield on bone biopsy in metastatic castration-resistant prostate cancer. *Prostate Cancer Prostatic Dis*. 2014;17:325-331.

10. Sailer V, Schiffman MH, Kossai M, et al. Bone biopsy protocol for advanced prostate cancer in the era of precision medicine. *Cancer.* 2018;124:1008-1015

11. Coleman RE. Clinical features of metastatic bone disease and risk of skeletal morbidity. *Clin Cancer Res*. 2006;12:6243s-6249s.

12. Perera M, Papa N, Christidis D, et al. Sensitivity, specificity, and predictors of positive (68)Ga-prostate-specific membrane antigen positron emission tomography in advanced prostate cancer: a systematic review and meta-analysis. *Eur Urol*. 2016;70:926-937.

13. Lecouvet FE, Oprea-Lager DE, Liu Y, et al. Use of modern imaging methods to facilitate trials of metastasis-directed therapy for oligometastatic disease in prostate cancer: a consensus recommendation from the EORTC Imaging Group. *Lancet Oncol.* 2018;19:e534-e545.

14. van Steenbergen TRF, Smits M, Scheenen TWJ, et al. (68)Ga-PSMA-PET/CT and diffusion MRI targeting for cone-beam CT-guided bone biopsies of castration-resistant prostate cancer patients. *Cardiovasc Intervent Radiol.* 2020;43:147-154.

15. Bins S, Cirkel GA, Gadellaa-Van Hooijdonk CG, et al. Implementation of a multicenter biobanking collaboration for next-generation sequencing-based biomarker discovery based on fresh frozen pretreatment tumor tissue biopsies. *Oncologist*. 2017;22:33-40.

16. Boellaard R, Oyen WJG, Giammarile F, et al. FDG PET/CT: EANM procedure guidelines for tumour imaging: version 2.0. *Eur J Nucl Med Mol Imaging.* 2015;42:328-354.

17. Shamonin DP, Bron EE, Lelieveldt BP, et al. Fast parallel image registration on CPU and GPU for diagnostic classification of Alzheimer's disease. Front Neuroinform. 2014;7:50.

18. Klein S, Staring M, Murphy K, Viergever MA, Pluim JP. Elastix: a toolbox for intensity based medical image registration. IEEE Trans Med Imaging. 2010;29:196-205

19. Lowekamp BC, Chen DT, Ibáñez L, Blezek D. The design of SimpleITK. *Front Neuroinform.* 2013;7:45.

20. Chakravarty D, Gao J, Phillips SM, et al. OncoKB: A precision oncology knowledge base. *JCO Precis Oncol*. 2017;2017.

21. Priestley P, Baber J, Lolkema MP, et al. Pan-cancer whole-genome analyses of metastatic solid tumours. *Nature*. 2019;575:210-216.

22. Van Dessel LF, van Riet J, Smits M, et al. The genomic landscape of metastatic castration-resistant prostate cancers using whole genome sequencing reveals multiple distinct genotypes with potential clinical impact. *Nat Commun.* 2019;10:5251.

23. Mermel CH, Schumacher SE, Hill B, Meyerson ML, Beroukhim R, Getz G. GISTIC2.0 facilitates sensitive and confident localization of the targets of focal somatic copy-number alteration in human cancers. Genome Biol. 2011;12:R41.

24. McLaren W, Gil L, Hunt SE, et al. The Ensembl Variant Effect Predictor. Genome Biol. 2016;17:122.

25. Harrow J, Frankish A, Gonzalez JM, et al. GENCODE: the reference human genome annotation for The ENCODE Project. *Genome Res*. 2012;22:1760-1774.

26. Martincorena I, Raine KM, Gerstung M, et al. Universal patterns of selection in cancer and somatic tissues. *Cell*. 2017;171:1029-1041.

27. R Core Team. R: A language and environment for statistical computing [computer program]. 2017. http//www.R-project.org/

28. Van der Velden DL, Hoes LR, Van der Wijngaart H, et al. The drug rediscovery protocol facilitates the expanded use of existing anticancer drugs. *Nature*. 2019;574: 127–131.

29. Paschalis A, Sheehan B, Riisnaes R, et al. Prostate-specific membrane antigen heterogeneity and DNA repair defects in prostate cancer. *Eur Urol*. 2019;76:469-478.

30. Wang B, Gao J, Zhang Q, et al. Diagnostic value of ^{68}Ga-PSMA PET/CT for detection of PTEN expression in prostate cancer: a pilot study. *J Nucl Med*. 2019; Epub ahead of print.

31. Thang S, Violet J, Sandhu S, et al. Poor outcomes for patients with metastatic castration-resistant prostate cancer with low prostate-specific membrane antigen (PSMA) expression deemed ineligible for ^{177}Lu-labelled PSMA radioligand therapy. *Eur Urol Oncol.* 2019;2:670-676

Figures and figure legends

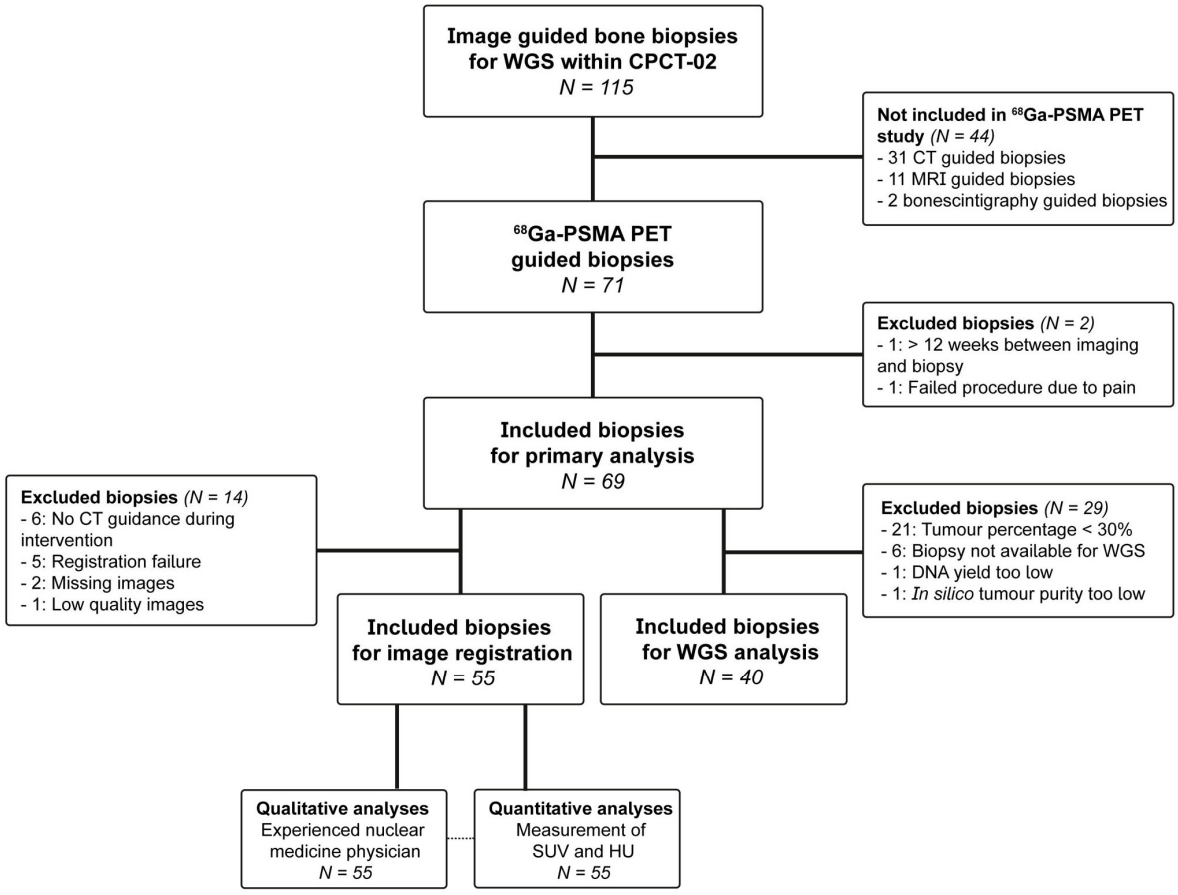

Figure 1 Flowchart of included ^{68}Ga-PSMA guided bone biopsies for primary and secondary analyses of the current PET study within CPCT-02. WGS: whole genome sequencing, SUV: standardized uptake value, HU: Hounsfield Units

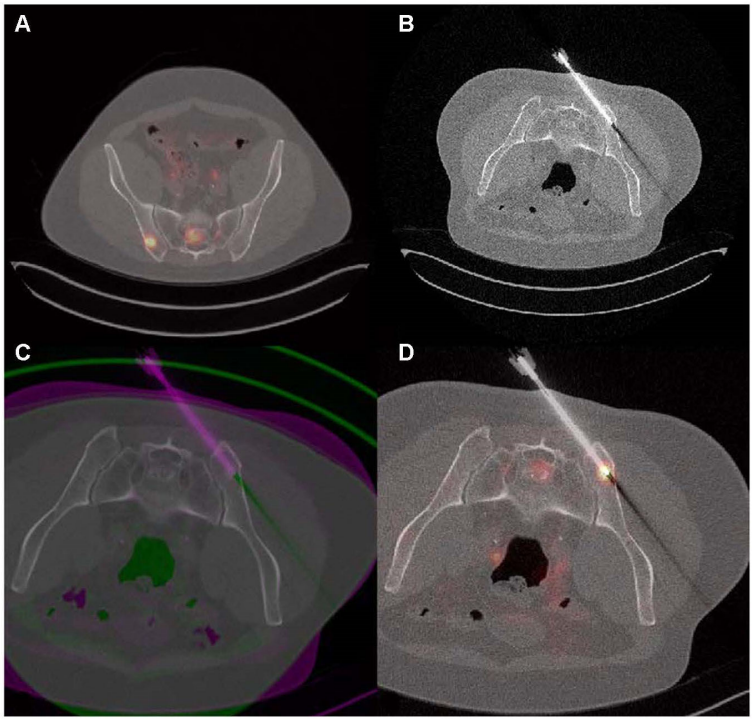

Figure 2 Rigid body image registration of ^{68}Ga-PSMA PET/CT and interventional CT visualizes biopsy needle on ^{68}Ga-PSMA PET and enables measurement of ^{68}Ga-PSMA uptake and radiodensity at biopsy site. A) ^{68}Ga-PSMA PET/CT, prior to the biopsy. B) CT, acquired during the biopsy procedure. C) Co-registration of ^{68}Ga-PSMA PET/CT and interventional CT. D) Visualization of biopsy needle on ^{68}Ga-PSMA PET/CT.

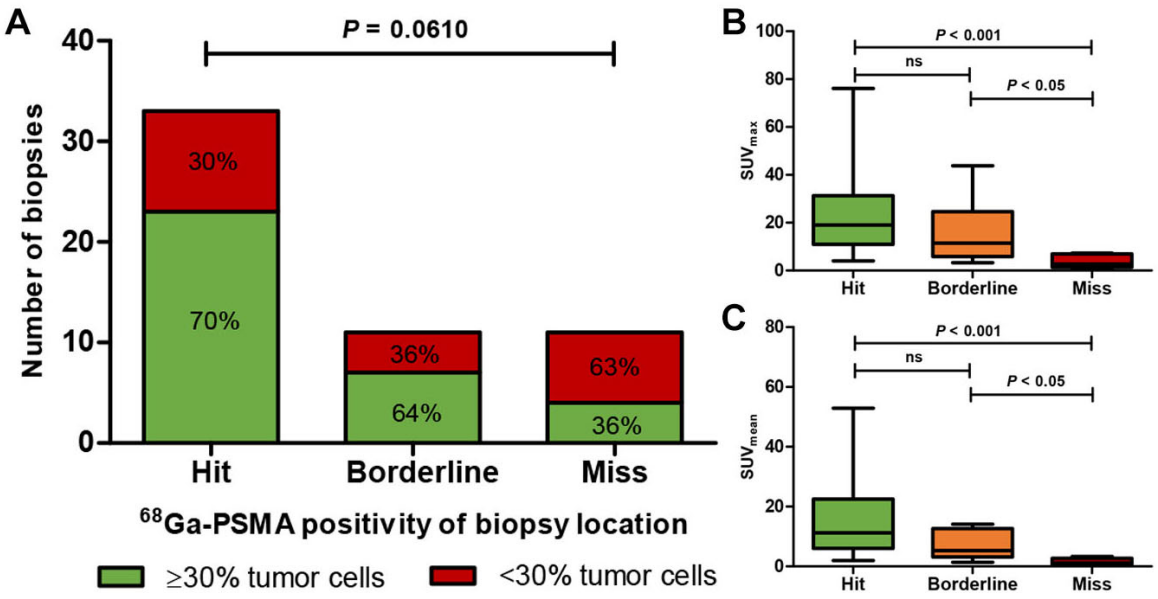

Figure 3 ^{68}Ga-PSMA uptake at biopsy sites A) Biopsy sites were categorized as hit (^{68}Ga-PSMA positive), borderline or miss (^{68}Ga-PSMA negative) by a blinded nuclear medicine physician and correlated to tumor percentage (≥30% vs <30%; N=55 biopsies). Chi-square for trend test. B) SUV_{max} at biopsy site, categorized by ^{68}Ga-PSMA uptake score (N=55 biopsies). Kruskal-Wallis in combination with Dunn's multiple comparisons test. C) SUV_{mean} at biopsy site, categorized by ^{68}Ga-PSMA uptake score (N=55 biopsies). Kruskal-Wallis in combination with Dunn's multiple comparisons test.

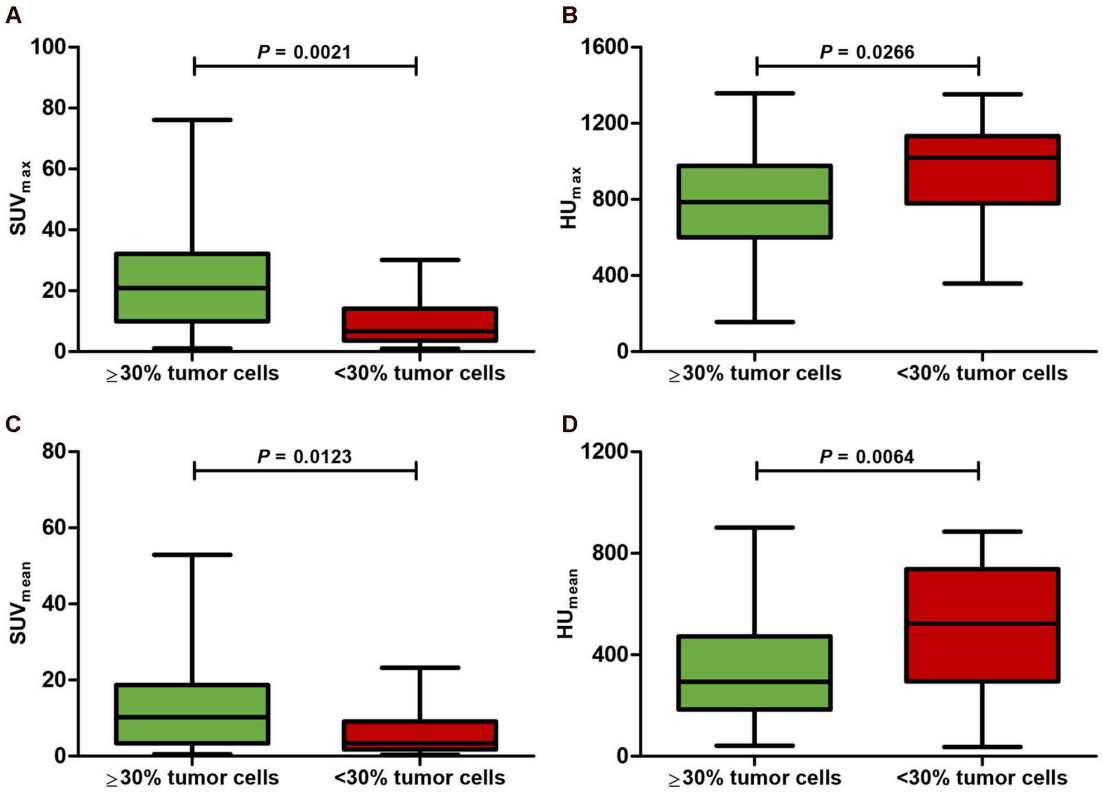

Figure 4 ^{68}Ga-PSMA uptake (SUV) and radiodensity (HU) in biopsies with tumor percentage ≥30% and <30%. A) SUV_{max}, B) SUV_{mean}, C) HU_{max}, D) HU_{mean}. N=55 biopsies. Mann Whitney test was performed for all parameters. SUV: standardized uptake values, HU: Hounsfield Units.

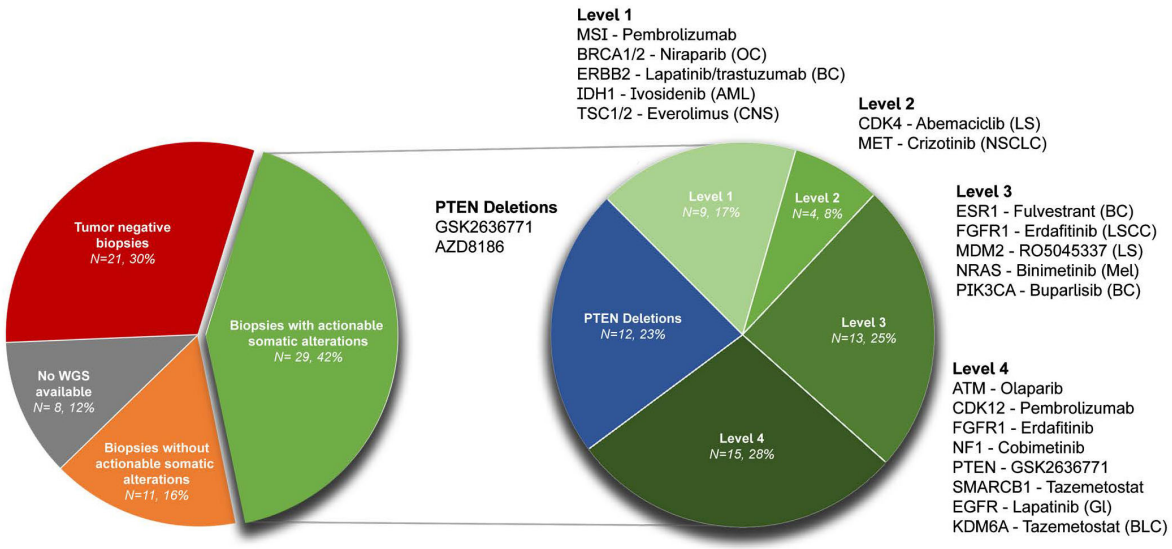

Figure 5 Actionable somatic alterations, detected by whole genome sequencing, in ^{68}Ga-PSMA PET guided bone biopsies from metastatic prostate cancer patients. Genes with actionable somatic alterations are categorized by level of evidence for targeted therapy as described in the OncoKB database. Evidence for both prostate cancer and other malignancies was combined within one category. Level 1: FDA-recognized biomarker predictive of response to an FDA-approved drug. Level 2: Standard care biomarker predictive of response to an FDA-approved drug. Level 3: Compelling clinical evidence supports the biomarker as being predictive of response to a drug. Level 4: Compelling biological evidence supports the biomarker as being predictive of response to a drug. For every altered gene, an example of a targeted therapy suitable for the specific alteration was described. WGS: whole genome sequencing, OC: ovarian cancer, BC: breast cancer, AML: acute myeloid leukemia, CNS: central nervous system cancer, LS: liposarcoma, NSCLC: non-small cell lung cancer, LSCC: lung squamous cell carcinoma, Mel: melanoma, Gl: glioma, BLC: bladder cancer.

Table 1 Clinical characteristics at time of biopsy

	^{68}Ga-PSMA guided bone biopsies (n= 69)	
Location of bone biopsy (n,%)		
Pelvis	57	82.6%
Spine	6	8.7%
Rib	3	4.3%
Extremity	3	4.3%
Location of bone biopsy irradiated (n,%)	3	4.3%
Age at biopsy (y) (mean ± SD)	68.5	± 8.3
Gleason score at primary diagnosis (n,%)		
<8	22	31.9%
≥8	39	56.5%
Unknown	8	11.6%
Prior local treatment (n,%)		
Radical prostatectomy	15	21.7%
External radiotherapy prostate	16	32.2%
Brachytherapy	1	1.4%
Hormone status at time of biopsy (n,%)		
mHSPC	2	2.9%
mCRPC	67	97.1%
Prior second generation ADT (n,%)		
Abiraterone	23	33.3%
Enzalutamide	34	49.2%
Prior chemotherapy (n,%)		
Docetaxel	49	71%
Cabazitaxel	19	27.5%
Estramustine	1	1.4%
Prior radiotherapy (n,%)		
Radium-223	5	7.2%
External radiotherapy metastatic site	21	30.4%
Laboratory values at time of biopsy (median, range)		
Haemoglobin (mmol/L) (n=67)	8.0	5.3 - 9.5
Leukocytes (x10^9/L) (n=62)	6.5	3.6 - 13.2
Thrombocytes (x10^9/L) (n=65)	232	122 - 576
Alkaline phosphatase (U/L) (n=59)	123	43 - 4598
LDH (U/L) (n=53)	233	152 - 2718
PSA (ug/L) (n=63)	96	0.14 - 2375

%; percentage of total number of biopsies with n = 69 biopsies; SD: standard deviation; mHSPC: metastatic hormone sensitive prostate cancer; mCRPC: metastastic castration resistant prostate cancer; ADT: androgen deprivation therapy; LDH: lactate dehydrogenase; PSA: prostate specific antigen.

Table 1 Clinical characteristics at time of biopsy Sixty-nine ^{68}Ga-PSMA PET guided biopsies from 60 individual patients were included. Seven patients underwent two biopsies during their treatment course. One patient underwent three biopsies during his treatment course.

Supplemental methods

Molecular analyses

Processing and analysis of whole-genome sequencing

We requested the whole-genome sequencing (WGS) data from the Hartwig Medical Foundation for prostate cancer patients (Erasmus MC and Radboud UMC) with bone metastasis who had successfully undergone a ^{68}Ga-PSMA guided biopsy and passed all pre- and post-WGS quality metrics (n = 40). These quality metrics consisted of a minimum tumor-cell percentage (≥30%) as estimated by an expert pathologist, sufficient DNA yield and an estimated *in silico* tumor-cell purity of at least 15%. Sample acquisition, library preparations, sequencing protocols and processing (alignment, QC, mutational calling, etc.) were performed as part of the CPCT-02 study and have been described previously*(1,2)*. In addition, GISTIC2 (v2.0.23)*(3)* was performed to determine recurrent and high-level amplifications/deletions of chromosomal regions:

gistic2 -b <output> -seg <segments> -refgene <hg19 UCSC> -genegistic 1 -gcm extreme -maxseg 4000 -broad 1 -brlen 0.98 -conf 0.95 -rx 0 -cap 3 -saveseg 0 -armpeel 1 -smallmem 0 -res 0.01 -ta 0.1 -td 0.1 -savedata 0 -savegene 1 -qvt 0.1

Furthermore, we re-annotated the somatic SNV, InDel and MNV variants with Variant Effect Predictor (VEP) using ENSEMBL annotations (ensembl-vep 95.1)*(4)* for GRCh37 and determined the overlap of genomic annotations based on GENCODE (v30)*(5)* on copy-number alterations (GISTIC2) and structural variants. Per somatic variant (on

nucleotide-level), we selected the most-deleterious coding effect per overlapping transcript; if a transcript had two or more coding mutations, these are summarized as “Multiple mutations”.

Identification of driver-genes and clinically actionable somatic events

Potential driver genes were determined by unbiased selection using dndscv (0.0.1.0)*(6)*, which detected genes under negative or positive mutational selection (qglobal_cv and/or qallsubs_cv ≤ 0.1) and by GISTIC2*(3)* focal copynumber-peak discovery on cohort-wide copy-number alterations (q ≤ 0.1) with GENCODE (v30) annotations*(5)*. This list of potential driver genes was complemented with detected driver genes based on the CPCT-02 pan-cancer study*(1)*. Structural variants potentially leading to known gene-fusions involving TMPRSS2, ETV, ERG or FLI1 were summarized as ETS fusions.

Somatic events (coding mutations, MSI, deep gain/deletions and structural variants) were reviewed in OncoKB*(7)* (version of June 21, 2019) to assess any clinically actionable events. All molecular analyses were performed with the statistical language platform R (v3.6.1)*(8)*.

Supplemental results

SUPPLEMENTAL TABLE 1a.

Univariate logistic regression analysis of biopsy outcome and significant continuous variables. N=55 biopsies.

Variable	p	Odds ratio	95% CI
SUV_{mean}	0.016	4.509	1.324-15,355
SUV_{max}	0.008	6.889	1.646-28.834
HU_{mean}	0.006	0.996	0.993-0.999
HU_{max}	0.037	0.998	0.995-1.000

SUPPLEMENTAL TABLE 1b.

Multivariate logistic regression analysis of biopsy outcome and significant continuous variables. N=55 biopsies.

Variable	p	Odds ratio	95% CI
SUV_{max}	0.003	11.737	2.258-60.996
HU_{mean}	0.003	0.995	0.992-0.998

Supplemental figures

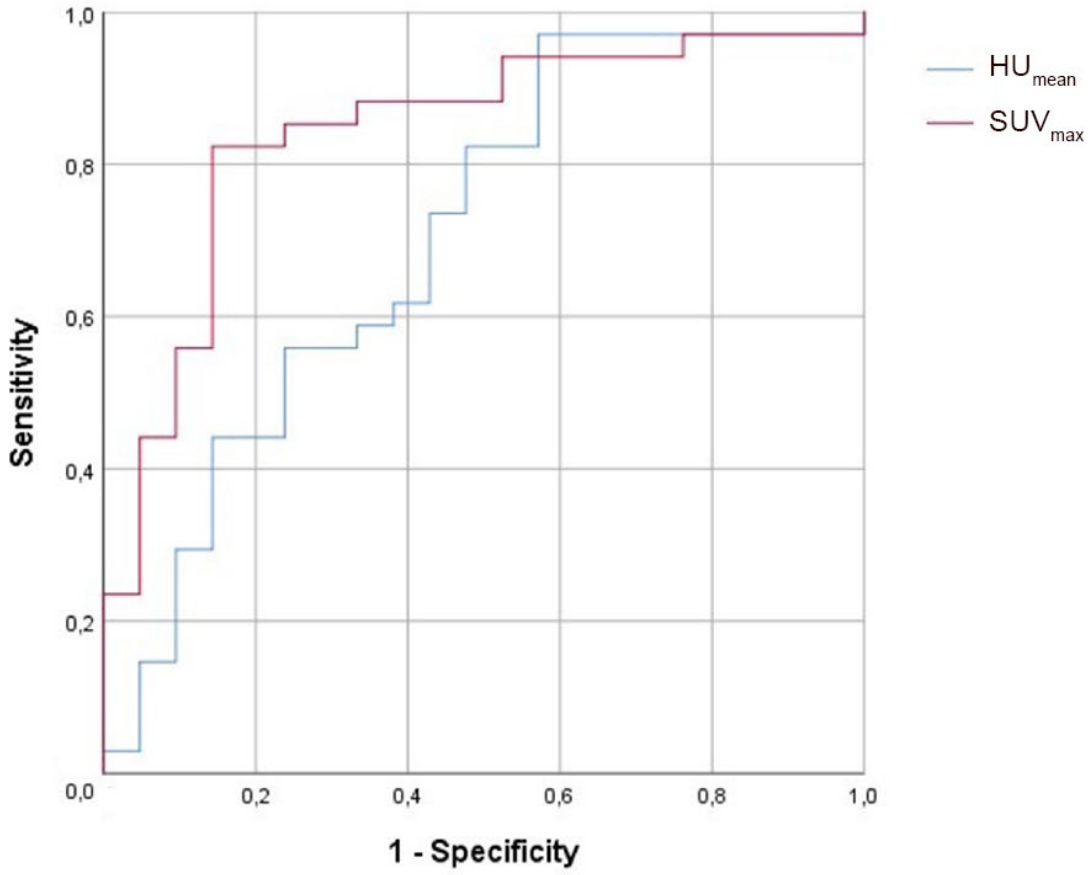

SUPPLEMENTAL FIGURE 1.

ROC curves for biopsy outcome by HU_{mean} and SUV_{max} at biopsy site. N=55 biopsies.


a
Tumor Cell Percentage
Tumor Cell Percentage
100%
75%
50%
25%
0%
0
.25
.5
.75
1
b
Mutations per Mb (Genome-wide TMB)
50
25
10
0
SNV
Indels
MNV
c
Structural variants
1000
500
250
100
10
Structural variants
d
Relative frequency
Structural variant categories
Translocation
Insertion
Inversion
Tandem Duplication (>100kb)
Tandem Duplication (<100kb)
Deletion (>100kb)
Deletion (<100kb)
e
Relative frequency
Ploidy status
0 1 2 3 4 5 6 7
f
Relative contribution Genome-wide
Mutational Signatures (COSMIC)
Age (Sig. 1 & 5)
AID/APOBEC (Sig. 2 & 13)
BRCA (Sig. 3)
MSI (Sig. 6, 15, 20, 21, 26)
DNA Polymerase η (Sig. 9)
Unknown aetiology
Filtered (<5%)
g
Relative Frequency
Mutational Changes (SNV)
C>A
C>G
C>T
T>A
T>C
T>G
h
Relative Frequency
Mutational Changes (DBS)
AC>NN
AT>NN
CC>AA
CC>NN
CC>TT
CG>NN
CT>NN
GC>NN
TA>NN
TC>NN
TG>NN
TT>NN
i
Genes
AR (n=23)
TP53 (n=17)
NKX3-1 (n=15)
PTEN (n=15)
FGFR1 (n=11)
PTPRD (n=8)
CHD1 (n=7)
KMT2C (n=7)
KMT2D (n=7)
CDKN1B (n=6)
FOXA1 (n=6)
BRCA2 (n=5)
RB1 (n=5)
APC (n=4)
DMD (n=4)
ERF (n=4)
MED12 (n=4)
NTRK1 (n=4)
SPOP (n=4)
CDK12 (n=3)
CIC (n=3)
CTNNB1 (n=3)
FOXQ1 (n=3)
GMDS (n=3)
GNA11 (n=3)
NF1 (n=3)
PIK3CA (n=3)
TOP2A (n=3)
ATM (n=2)
ARHGAP1 (n=2)
IDH1 (n=2)
0% 25% 50% 75% 100%
dN/dS
GISTIC2
j
Chromothripsis
k
Kataegis
l
ETS Fusion
Coding mutations
Structural variants
Deep Amplifications
Deep Deletions
PSMA Cohort (n = 40)
Frameshift Variant
Inframe Insertion/Deletion
Synonymous Variant
Missense Variant
Multiple Mutations
Neutral
Splice Donor Variant
Stop Gained
Structural Variant
Shallow Deletion
Deep Deletion
Shallow Gain
Deep Gain

SUPPLEMENTAL FIGURE 2.

Mutational landscape of ^{68}Ga-PSMA guided bone biopsies identified by whole-genome sequencing.

A) Estimated tumor cell percentages (*in silico*) obtained from the whole-genome sequencing data. Bars are color-coded based on tumor cell percentage.

B) Number of genomic mutations per Mbp (TMB) of SNV, InDels, and MNV categories. All genome-wide somatic mutations were taken into consideration (square root scale). C) Absolute number of unique structural variants per sample. Cumulative frequency of inversions, tandem duplication, deletions, insertions, and translocations.

D) Relative frequency per structural variant category. Tandem Duplications and Deletions are subdivided into >100 kbp and <100 kbp categories. This track shows whether enrichment for a particular category of (somatic) structural variant can be detected, which in turn, can be indicative for a specific mutational aberration.

E) Relative genome-wide ploidy status, ranging from 0 to ≥7 copies. This track shows the relative percentage of the entire genome which is (partially) deleted (ploidy < 2/diploid) or amplified (> 2/diploid).

F) Relative contribution to mutational signatures (COSMIC) summarized per proposed etiology. This track displays the proposed etiology of each SNV based on their mutational contexts. Signatures with < 5% relative contribution in all samples were summarized in the “Filtered (<5%)” category.

G) Relative frequency of somatic Single Nucleotide Variants (SNV) categories.

H) Relative frequency of somatic Doublet Base Substitution (DBS) categories.

I) Oncoplot showing the somatic mutations per samples for a selection of potential driver genes, as detected by dN/dS and/or GISTIC2 analysis and/or manual selection based on

a list of pan-cancer (CPCT-02) driver genes[1]. Shallow amplifications and deletions are only shown if also accompanied by an additional coding mutation. The right-hand bar-plot depicts the relative frequency of mutational categories (coding mutations, structural variants and deep amplifications/deletions) per gene. Per gene, the inclusion criteria are shown; dN/dS (q≤0.1; *), enriched GISTIC2 focal peak (q ≤ 0.1; †) or if empty, based on the pan-cancer (CPCT-02) driver list.

J) Presence of chromothripsis. Pink color indicates presence of chromothripsis as estimated by ShatterSeek.

K) Presence of kataegis. Red color indicates presence of one or more regions showing kataegis.

L) Presence of a fusion with a member of the ETS transcription factor family. Green color indicates a possible fusion.

Supplemental references

1. Priestley P, Baber J, Lolkema MP, et al. Pan-cancer whole-genome analyses of metastatic solid tumours. *Nature*. 2019;575:210-216.

2. Van Dessel LF, van Riet J, Smits M, et al. The genomic landscape of metastatic castration-resistant prostate cancers using whole genome sequencing reveals multiple distinct genotypes with potential clinical impact. *Nat Commun.* 2019;10:5251.

3. Mermel CH, Schumacher SE, Hill B, Meyerson ML, Beroukhim R, Getz G. GISTIC2.0 facilitates sensitive and confident localization of the targets of focal somatic copy-number alteration in human cancers. Genome Biol. 2011;12:R41.

4. McLaren W, Gil L, Hunt SE, et al. The Ensembl Variant Effect Predictor. Genome Biol. 2016;17:122.

5. Harrow J, Frankish A, Gonzalez JM, et al. GENCODE: the reference human genome annotation for The ENCODE Project. *Genome Res*. 2012;22:1760-1774.

6. Martincorena I, Raine KM, Gerstung M, et al. Universal patterns of selection in cancer and somatic tissues. *Cell*. 2017;171:1029-1041.

7. Chakravarty D, Gao J, Phillips SM, et al. OncoKB: A precision oncology knowledge base. *JCO Precis Oncol*. 2017;2017.

8. R Core Team. R: A language and environment for statistical computing [computer program]. 2017. http//www.R-project.org/